ACS APPLIED MATERIALS & INTERFACES

Research Article

www.acsami.org

# A Facile Method to Prepare Molecularly Imprinted Layer-by-Layer Nanostructured Multilayers Using Postinfiltration and a Subsequent Photo-Cross-Linking Strategy

Yong Zhou,[†] Mengjiao Cheng,[†] Xiaoqun Zhu,[†] Yajun Zhang,[†] Qi An,*[,‡] and Feng Shi*[,†]

[†]State Key Laboratory of Chemical Resource Engineering & Key Laboratory of Carbon Fiber and Functional Polymer, Ministry of Education, Beijing University of Chemical Technology, Beijing 100029, China

[‡]School of Materials Science and Technology, China University of Geoscience (Beijing), Beijing 100083, China

Supporting Information

**ABSTRACT:** In this paper, we have demonstrated a facile strategy to prepare molecularly imprinted layer-by-layer nanostructured films. This strategy has circumvented the requirement of using photocross-linkable polymers, which suffered from tedious synthetic processes in the construction of surface molecular imprinting in layer-by-layer (SMI-LbL) devices. The described SMI-LbL device was constructed by employing the traditional construction procedures of LbL systems, followed by the postinfiltration of bifunctional photosensitive cross-linking agent 4,4′-diazostilbene-2,2′-disulfonic acid disodium salt into the prepared multilayers, and subsequent photocross-linking. A robust SMI-LbL device with high fatigue-resistance was achieved. The preparation conditions have been optimized to achieve repeated unloading and rebinding of the targeting molecule with high fidelity. The combination of templating and cross-linking is the core factor to achieve high fidelity and high efficiency of the SMI-LbL device.

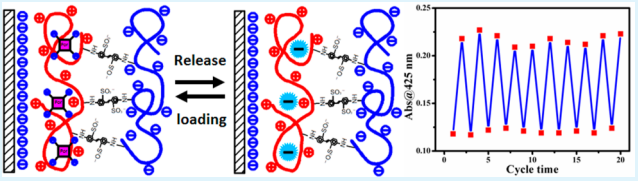


**KEYWORDS:** *surface molecular imprinting, layer-by-layer, photo-cross-linking, diazostilbene, self-assembly, supramolecular*

## INTRODUCTION

Molecularly imprinted polymers (MIP) provide general and versatile means to generate specific binding sites in polymer matrices, and this technique has been widely employed in sensor matrices and separation materials. Despite its wide range of applications, it suffers from limitations associated with the limited accessibility to the imprinted sites, and the long diffusion paths required as a result of the bulk volume of the polymer.[1] In order to shorten the diffusion path of the targeted molecules and further enhance the proportion of the accessible binding sites, surface MIP devices were developed, where the MIPs were constructed on the surfaces or interfaces of various substrates such as electrodes,[2−5] photonic crystal devices,[6−8] and hierarchichal porous matrices for the construction of sensors with advanced detection capabilities.[9] Surface molecular imprinting in layer-by-layer (SMI-LbL) nanostructured films is a facile strategy to construct surface MIPs. The concept of SMI-LbL was first introduced by Zhang and co-workers[10] in 2007, and underwent rapid development thereafter. The technique requires the formation of the imprinting complex in solution, and subsequent construction of the imprinted multilayers by the LbL technique and interlayer cross-linking. Once the imprinted template is extracted from the multilayers, the device prepared has the capability to load targeted molecules with high loading efficiency and high reproducibility. The mechanism for the superior capabilities of the SMI-LbL technique has been confirmed; the majority of template uptake is due to selective binding into imprinted sites.[11] Due to its special merits, this technique has received significant attention in recent years, for construction of advanced devices for separation, detection, and nanofabrication. Various specific interactions for formation of the imprinting complex were explored, including electrostatic interactions, hydrogen-bonding, and even labile covalent bonding, aiming to promote the imprinting efficiencies of the complex for a variety of templating molecules.[12,13] To further explore its potential applications, the technique of SMI-LbL has been integrated with other diverse nanotechniques to achieve advanced devices. These include: employing an SMI-LbL film in the microcontact printing technique for enhancement of the charge selectivity of the imprinted-film-modified stamp;[14] combination with porous membranes to obtain selective filtration devices;[15] and integration with nanoparticles to render a device with an even larger proportion of active surface areas.[16] In all the above-mentioned systems, cross-linking of the LbL polymer has remained the core of the technique, and allows the multilayers of sufficient rigidity and with reproducible loading. However, despite the versatility of the SMI-LbL technique and its wide integration with other nanotechniques, the construction units of SMI-LbL have been narrowly restricted due to the requirement of cross-linking to two LbL systems. One strategy is using photoactive diazoresin (DAR) and its negatively charged counterpart polymers as building blocks to

Received: November 19, 2012
Accepted: August 7, 2013
Published: August 7, 2013

  

Scheme 1[a]

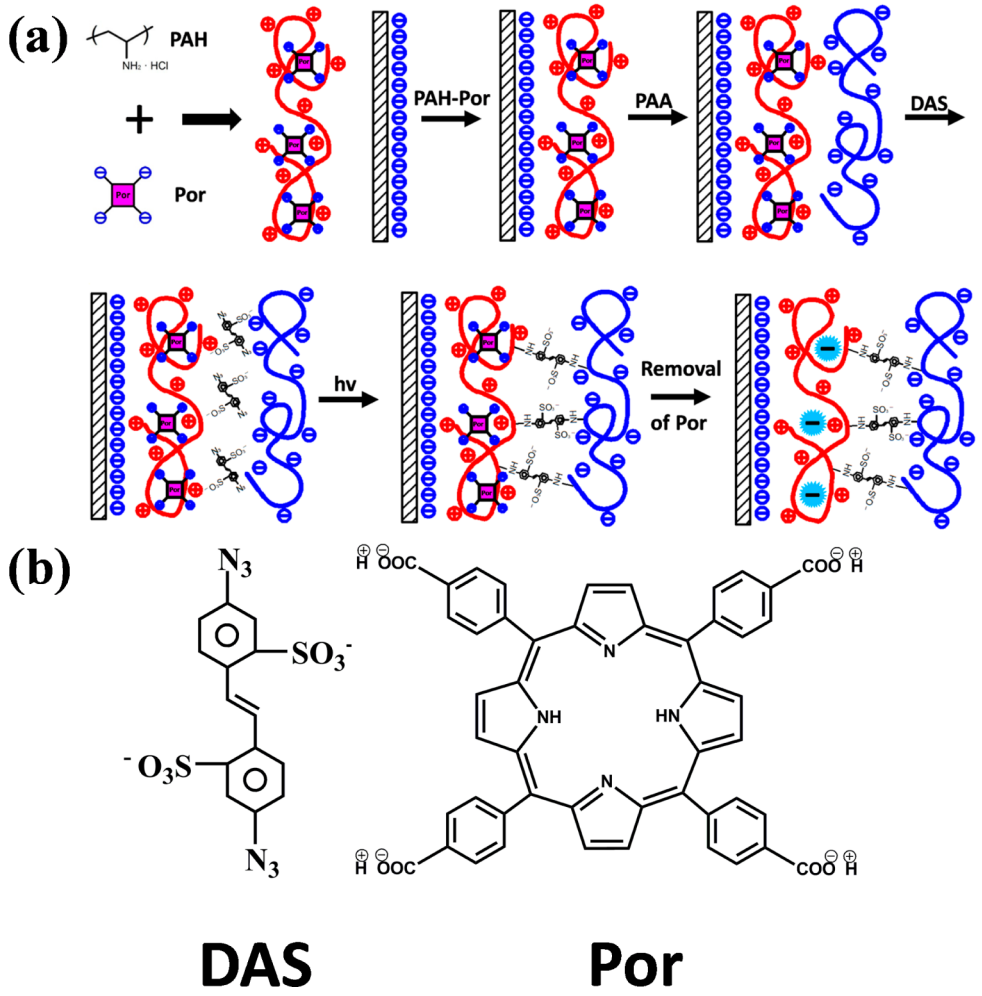


[a](a) Illustration of the construction of the molecularly imprinted LbL nanostructures by using the postinfiltration and subsequent photo-cross-linking strategy. (b) Molecular formula of the bifunctional photosensitive molecule DAS and the templating molecule Por.

construct SMI-LbL multilayers after UV cross-linking; the other is constructing SMI-LbL multilayers from polymers grafted with thiol groups and then cross-link the LbL system through the formation of disulfide bonds upon oxidation. This special demand has significantly compromised the convenience and versatility provided by traditional LbL techniques. It could be tedious to synthesize intended polymers grafted with phenyl azido groups or thiol groups. Thus, developing novel construction methods to circumvent the use of DAR or polymers with thiol function groups in SMI-LbL devices would further enhance the potential applications of the SMI-LbL system. This has, however, remained a long-standing challenge in the development of the SMI-LbL technique. To address this challenge, we report a novel strategy to prepare an SMI-LbL system, by employing traditional construction procedures of LbL systems followed by the postinfiltration of bifunctional small molecules into the prepared multilayers, and then cross-linking the multilayer through the formed nitrenes under UV irradiation. We employ the composite of poly(allylamine hydrochloride) (PAH) and meso-tetra(4-carboxyphenyl)-porphine (Por) as the positive building block (PAH-Por) and poly(acrylic acid) (PAA) as the counter negatively charged building block, to fabricate multilayers with repeated molecular imprinting and extraction capabilities. 4,4′-Diazostilbene-2,2′-disulfonic acid disodium salt (DAS) was chosen as the postinfiltrated photosensitive molecule, because the diazo group forms covalent bonds with a broad range of functional groups under UV irradiation, and thus maintains the opportunity of its compatibility with diverse traditional LbL systems. To the best of our knowledge, this is the first demonstration of a robust SMI-LbL device achieved with traditional LbL construction methods, followed by its stabilization by postinfiltration of cross-linkable bifunctional small molecules and photoirradiation.

## MATERIALS AND METHODS

**Materials and Instruments.** PAA, $M_w$ = 240 000 g/mol, 25 wt %, poly(diallyldimethylammonium chloride), PAH, $M_w$ = 15 000 g/mol, Por, (3-mercaptopropyl)-trimethoxysilane (MPTS), tetrakis (4-(trimethylammino)-phenyl-21H, 23H-porphine, tetratosylate (Por-$NH_3^+$), 3-mercaptopropionic acid (MPA), and DAS were purchased from Sigma-Aldrich. Sodium hydroxide, hydrogen chloride, hydrogen peroxide (30 wt %), and sulfuric acid were purchased from the Beijing Chemical Reagent Company (Beijing, China). Quartz substrates were purchased from the Changchun Institute of Optics, Fine Mechanics and Physics, Chinese Academy of Sciences. UV−visible spectra were obtained on a Hitachi U-3900 spectrophotometer. Atomic force microscopy (AFM) images were obtained from a Dimension 3100


dx.doi.org/10.1021/am4023626 | ACS Appl. Mater. Interfaces 2013, 5, 8308−8313

instrument, from Veeco. Electrochemical experiments were performed on a CHI660e electrochemical workstation (Chenhua, Shanghai).

**Surface Modification of Quartz Substrates.** The self-assembled monolayer of sulfonic groups was formed by the following procedure: (1) the quartz substrate was cleaned by immersing it in Piranha solution ($H_2SO_4/H_2O_2$ (v/v) 7:3) for 1 h, washing thoroughly with distilled water, and drying with $N_2$, leading to a hydrophilic surface covered with −OH groups; (2) the cleaned substrate was immersed in a toluene solution of MPTS ($1 \times 10^{-5}$ M) for 12 h, and resulted in a monolayer of mercapto groups; and (3) the substrate modified with mercapto groups was treated with a mixed solution of 30% $H_2O_2$/acetic acid (v/v = 1:5) at 50 °C for 1 h to oxidize the mercapto groups to sulfonic groups.

**Preparation of LbL Multilayers and Their Photoreaction.** Aqueous solutions of PAA, PAH, and Por with concentrations of 1 mg/mL were prepared separately, and their pH values were adjusted to 6 by HCl and NaOH. At this pH value, Por is negatively charged and PAH is positively charged. An aqueous solution of DAS was prepared with a concentration of 5 mg/mL at a pH of 3.8 adjusted by HCl. The complexes of PAH and Por were prepared by slowly dropping Por solution using a syringe into PAH solution under ultrasonication, and the resulting volume ratio of PAH and Por is 5:1.

The quartz substrate modified with sulfonic groups was alternately and repeatedly immersed into the aqueous solution of PAH-Por for 20 min and the aqueous solution of PAA for 20 min. Between each step, the substrate was thoroughly washed with large volumes of deionized water and then dried with $N_2$. In total, 7.5 cycles of LbL construction were conducted for each substrate, keeping PAH-Por as the outmost layer unless otherwise stated.

After the construction of $(PAH\text{-}Por\text{-}PAA)_{7.5}$ multilayers, cross-linked multilayers were constructed by postinfiltration of DAS into the multilayers for 1.5 h, followed by photoactivation with a 400 W high-pressure mercury lamp from a distance of 20 cm with an intensity of 2.5 mW·cm$^{-2}$ for 20 s. The process of the construction of the molecularly imprinted multilayers is illustrated in Scheme 1.

**The Removal and Rebinding of Por.** The binding sites within the cross-linked $(PAH\text{-}Por/PAA)_{7.5}$ multilayers were generated through removal of Por from the films, by immersing the modified substrates into an aqueous solution of sodium hydroxide (pH = 12.5) for 30 min, followed by washing with deionized water and drying with $N_2$. Readsorption of Por was completed by rinsing the substrate in an aqueous solution of Por (1 mg/mL) for 30 min, followed by washing with deionized water to remove nonspecifically adsorbed Por.

**Electrochemical Measurements.** The electrochemical measurement required a clean and negative-charge-bearing electrode surface. The gold electrodes were first mechanically polished with 1 and 0.3 $\mu$m $\alpha$-$Al_2O_3$ and washed ultrasonically with deionized water; afterward, they were electrochemically scanned in a 2 mM $K_3[Fe(CN)_6]$ and 0.1 M KCl solution by potential scanning between −0.2 and 0.8 V with the scanning rate of 0.1 V/s until a reproducible cyclic voltammogram was obtained. Subsequently, the gold electrode was modified in an ethanol solution of MPA ($1 \times 10^{-4}$ M) for 12 h and fabricated SMI-LbL with the same buildup methods as that on quartz substrates.

Electrochemical experiments were carried out in a conventional three-electrode glass electrochemical cell. A gold electrode modified with a PAH-Por/PAA multilayer was used as the working electrode. The auxiliary electrode was platinum, and the reference electrode was an Ag/AgCl (saturated KCl) electrode. The experiments were performed at ambient temperature. The cyclic voltammetry scanning (CV) was carried out in a mixed solution of 2 mM $K_3[Fe(CN)_6]$ and 0.1 M KCl solution, with scanning potential between −0.2 and 0.8 V at a scanning rate of 0.1 V/s until a reproducible cyclic voltammogram was obtained.

## RESULTS AND DISCUSSION

**Formation of the (PAH-Por) Imprinting Complex.** Por was selected as the template molecule in MIP for the following reasons: first, it has multiple negative charges, making it easy to form composite with PAH; second, it shows strong UV absorption, which is easy to be tracked by the UV−visible spectrum; third, it has a specific planar molecular geometry to form an imprinted site. All of the above factors were expected in the fabrication of MIP system, and they were the main reason for selecting Por as the template molecule in most reported SMI-LbL.[5,8,9] At a pH value of 6, the weak electrolyte PAH was positively charged due to its partial ionization and Por was negatively charged. Thus, they could form the imprinting complex driven by electrostatic attractions, and the complex of PAH-Por exhibits a positive charged property because the mole ratio of PAH and Por is about 42. Compared with the absorbance of the aqueous solution of Por, the absorbance band for the multilayers is red-shifted by around 10 nm (Figure 1 and Supporting Information Figure S1). This complex of PAH-Por then electrostatically interacted with PAA to construct multilayers during the LbL process.

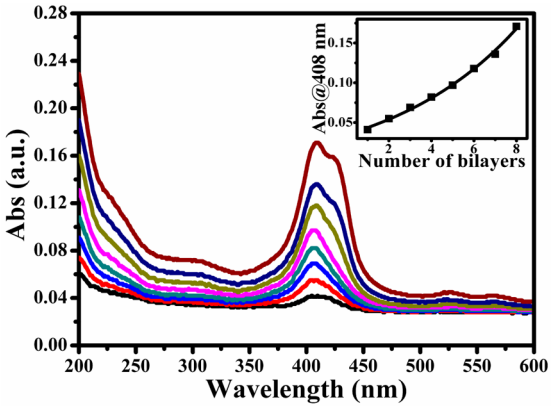


**Figure 1.** UV−visible spectra of $(PAH\text{-}Por/PAA)_n$ ($n$ = 1−7.5), measured after each bilayer was fabricated. The inset shows the intensities of absorption of PAH-Por at 408 nm in relation to the number of bilayers.

**Preparation of SMI-LbL Self-Assembled Films.** Because the PAH/PAA multilayer films were widely used in LbL constructions, we chose this system as the model to demonstrate our strategy. The stepwise assembly of PAH-Por and PAA were followed by measuring the characteristic absorbance band of Por at around 408 nm. We observed an exponential increase of the absorbance intensities of Por during the construction of multilayers (Figure 1). The equilibrium adsorption time of PAH-Por was experimentally determined as 90 s, but to ensure optimized adsorption, we adopted an immersion time of 20 min in the experiments (Figure S2, Supporting Information). To study whether the inclusion of Por into PAH influenced the construction of the well-studied (PAH/PAA) multilayers, we compared the construction process of $(PAH\text{-}Por/PAA)_{7.5}$ and $(PAH/PAA)_{7.5}$ multilayers (Figure S3, Supporting Information). The similarity of the growth processes between the two systems indicated that the existence of Por did not influence the build-up of the multilayers significantly; both systems showed exponential increase of absorbance in relation to the number of bilayers, with an acceleration observed from the fourth bilayer to the seventh bilayer.

**Rigidifying the Multilayers by Postinfiltration and Photochemical Cross-Linking.** In order to rigidify the multilayers and facilitate the subsequent extractions and rebindings of Por, cross-linking of the multilayers by post-

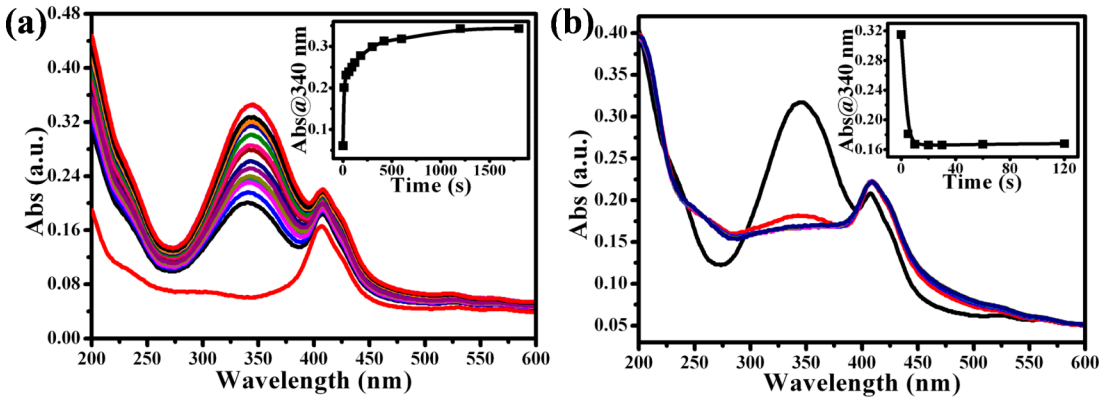


**Figure 2.** (a) UV−visible spectra taken during the process of diffusing DAS into the multilayers. Inset: absorbance at 340 nm as a function of time during the diffusion of DAS into the $(PAH\text{-}Por/PAA)_{7.5}$ multilayers. (b) UV−visible spectra of multilayers in the process of UV irradiation. Inset: absorbance intensities at 340 nm decrease as the amount of DAS in the multilayers decreases.

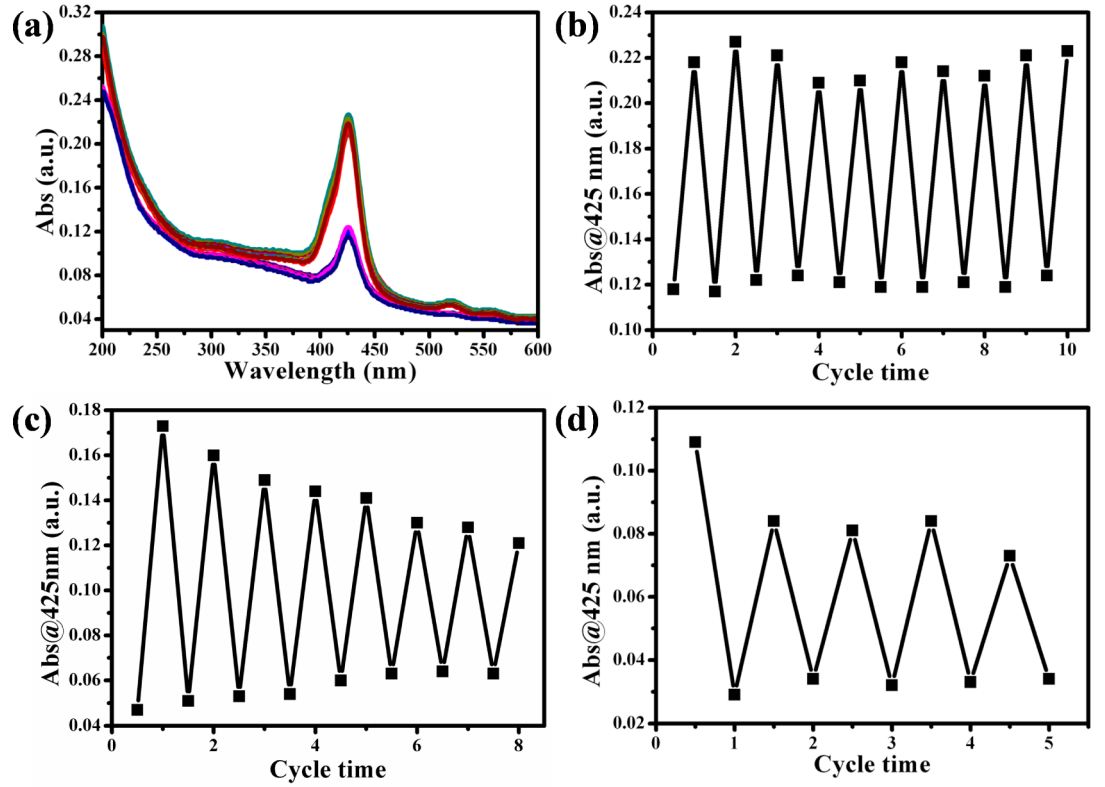


**Figure 3.** (a) UV−vis spectra of cross-linked $(PAH\text{-}Por/PAA)_{7.5}$ during repeated extraction and reloading of the template molecule Por. (b) Absorbance intensities of cross-linked $(PAH\text{-}Por/PAA)_{7.5}$ at 425 nm following each extraction and reloading step. (c) Absorbance intensities of $(PAH\text{-}Por/PAA)_{7.5}$, without cross-linking, at 425 nm following each extraction and reloading step. (d) Absorbance intensities of cross-linked $(PAH/PAA)_{7.5}$, without incorporation of template Por, at 425 nm following each extraction and reloading step.

infiltration of the cross-linker and subsequent reaction were conducted. The strategy of cross-linking should meet key requirements, such as (i) the cross-linker should be a bifunctional molecule that forms covalent bonds with both PAH and PAA polyelectrolyte; (ii) the postinfiltration process is efficient, and little damage to the imprinted PAH-Por/PAA multilayers should be caused by the process, and (iii) the reaction conditions for cross-linking should specifically induce the intended reactions to take place with facile control over timing and energy, without disturbing the whole system by introducing unnecessary additional energy.

To this end, we chose DAS as the bifunctional cross-linker, and initiated the reactions with photochemical irradiation. DAS was first diffused into the multilayers (PAH-Por/PAA). The diffusion process was followed by UV measurement and the peak intensity at 340 nm, corresponding to the maximum absorbance of DAS, was plotted as a function of time (Figure 2a). The amount of DAS absorbed in the multilayers increased with time in the early stage, and remained almost constant after 20 min, indicating the amount of DAS in the multilayers was at equilibrium with the amount of DAS in solution. We chose 1.5 h as the diffusion time, to ensure thorough diffusion of DAS into the multilayers in the fabrication of the molecularly imprinted functional film. The maximum loaded amount of DAS was calculated to be 0.08 $\mu g \cdot cm^{-2} \cdot layer^{-1}$. During the process of infiltration, the characteristic absorbance of Por


dx.doi.org/10.1021/am4023626 | ACS Appl. Mater. Interfaces 2013, 5, 8308−8313

remained unchanged, indicating that the structure of the multilayers with imprinted Por was not disturbed, following observation that no measurable loss of Por was detected.

Following the diffusion process, photochemical cross-linking was carried out. The decrement of DAS was evident by the decrease of its characteristic absorbance, as shown in Figure 2b. With photo irradiation, the azido groups in DAS can be decomposed into highly reactive nitrene intermediates with released nitrogen. The nitrene can be introduced into the C−H or N−H bonds and form interlayer and intralayer photocross-links (Scheme 1).[17] As a result, covalently cross-linked three-dimensional multilayers were obtained with higher rigidity, as verified in the following section. The photo-cross-linking process was completed within 20 s. During the photochemical reaction, the absorbance around 340 nm decreased with elongation of the irradiation period, and associated increases in the vicinity of 270 and 415 nm were observed. This phenomenon is consistent with the photochemical reaction of DAS. The absorbance from 200−250 nm and from 550−600 nm was unchanged, and shape of the absorbance band corresponding to Por was unchanged. These phenomena indicate that the imprinted Por in multilayers were not disturbed during the UV irradiation process. To further confirm this issue, we used AFM to characterize the surface morphologies of the multilayers before and after the photo-cross-linking. From the AFM images in Figure S4 in the Supporting Information, we can see clearly that both of the multilayers presented similar surface morphology, indicating that the multilayers were not disturbed by the process of infiltration and photochemical reactions.

**Reproducible Extraction and Recognition of the Surface Imprinted Multilayers.** The as-prepared SMI-LbL systems showed highly reproducible unloading and recognition ability toward the template molecule Por. After photo-cross-linking of the multilayers, Por was removed from the polymer film by immersing the substrate into an aqueous solution of sodium hydroxide. The solution of sodium hydroxide was used to extract Por because it could deionize PAH and effectively break the electrostatic interactions between Por and PAH. The efficient removal of Por was evident by the disappearance of its characteristic absorption in the polymer film (Figure 3a). Then, immersion of the multilayers into an aqueous solution of Por recovered the absorbance spectrum of Por, indicating the rebinding of the molecule. The rebinding event reached equilibrium within 5 min for every tested concentration (Figure S5, Supporting Information). The binding constant between Por and the imprinted multilayers was determined as $6.03 \times 10^5$ $M^{-1}$, by plotting the change of intensity at 425 nm (characteristic of Por) as a function of the bulk concentrations of Por, and fitting the data points to the Langmuir isotherm (Figure S6, Supporting Information).[18] This value was estimated to be at least 10 times larger than the affinity between Por and the unimprinted multilayers (Figure S7, Supporting Information). High fidelities of repeated extractions and rebinding abilities were achieved, as shown in Figure 3a and b. Even after 10 cycles of extraction and readsorption, the absorbance intensity of Por was almost identical to that of the original film before the first extraction process. During the repeated extraction process, fluctuations of the differences in absorbance existed for the loading−unloading status between 0.085 and 0.11. The fluctuation was considered to be within experimental errors, and both the absolute difference, around 0.1, and fluctuation, of 0.025, were repeatable for different devices. Thus, the constructed devices were considered to work with high fidelity. This high level of fidelity indicated that the covalently cross-linked SMI-LbL device, as constructed, is stable under the extraction and reloading conditions and displayed satisfactory fatigue resistance. We speculate that the covalent cross-linking process is indispensible for the excellent stability of the device. To verify our speculation, control polymer films without cross-linking were prepared. In these control films, the reloading capability decreased rapidly as the extraction−reloading cycles proceeded. After 8 cycles, the absorbance intensity reached only 60% of the original value (Figure 3c). This rapid decrease of reloading capacity of the control film could be due to two possible reasons. One is the relaxation of the polymer chains after repeated washing and immersion steps. The other is the possible loss of the electrolyte polymers of PAH or PAA from the substrates into the bulk solution. This control experiment highlighted the importance of covalent cross-linking, and thus the indispensible role of DAS in the construction of fatigue-resistant SMI-LbLs.

Furthermore, the indispensible role of molecular imprinting to achieve a high loading capacity was proved by a second control experiment, where the multilayers were assembled without adding Por as the template molecule. The Por capacity of these multilayers was only 44% of that of the imprinted and cross-linked multilayers after 5 cycles of unloading and reloading (Figure 3d). This result is consistent with previous reports that, despite the universal existence of electrostatic interactions between electrolyte multilayers and small molecules, the introduction of a molecular template is a key factor in achieving high loading efficiency in SMI-LbL devices. The experimental proofs herein verified that the SMI-LbL device, constructed by the conventional LbL method followed by postinfiltration and cross-linking, displayed advanced extraction and reloading capacity toward the targeted molecule, with the combination of templating and cross-linking as core factors to achieve the high fidelity and high efficiency of the device.

**CV Characterization of Competitive Adsorption of Por and Redox Label into the SMI-LbL Device.** In order to clarify that the imprinting of Por molecules is the cooperation effects of electrostatic interactions and specific imprinted sites, we characterized the competitive adsorption of Por and Por-$NH_3^+$ by the electrochemical probing of the association of the negatively charged $[Fe(CN)_6]^{3-}$ label to the polymeric film before and after exclusion of the template Por from the polymer. From Figure S8 in the Supporting Information, we can observe that the redox response for the $[Fe(CN)_6]^{3-}$ is decreasing remarkably when the polymeric film is loaded with the template Por, implying that the reloaded Por prevents the interfacial electron transfer to the redox-label. However, when replacing the Por solution with Por-$NH_3^+$, we can observe that, after immersing in a mixed solution of 0.5 mg/mL Por-$NH_3^+$, 2 mM $K_3[Fe(CN)_6]$, and 0.1 M KCl for 20 min, the redox response for the $[Fe(CN)_6]^{3-}$ changes not significantly, as shown in Figure S9 in the Supporting Information. This phenomenon is attributed to the fact that the imprinted sites in the film can accommodate Por through electrostatic interactions, in addition to its sterical adaption to the imprinted multilayer. These two effects contribute synergistically to the stabilization of Por in the imprinted film.

## CONCLUSION

In this study, we reported a novel approach to generate surface molecular imprinting devices with polymeric films, which

combined traditional LbL construction and post photochemical cross-linking of the layered multilayers. The post diffusion of cross-linking agent DAS serves as a versatile approach to covalently cross-link polymer layers. This reported strategy frees the construction unit of SMI-LbL devices from the requirement of being photochemically cross-linkable. With the introduction of new chemistry in the area of SMI-LbL construction, it is reasonable to expect abundant possibilities for the construction of SMI-LbL multilayers from diverse polymers, making the facile concept of SMI-LbL wildly applicable. This strategy is expected to find applications in devices for selective filtration, separation, nanoreactors, and sensors. Currently, the thermodynamics and kinetics of the adsorption of the targeted molecule, in addition to its selectivity in mixed solution, is under investigation. The possible applications of the chemistry when introduced to different electrolyte construction pairs are also being explored.

## ■ ASSOCIATED CONTENT

### Ⓢ Supporting Information

UV−visible spectrum of the aqueous solution of Por, absorption kinetics of the complex PAH-Por, UV−visible spectra of the build up process of $(PAH/PAA)_{7.5}$, AFM images for the $(PAH\text{-}Por/PAA)_{7.5}$ multilayer before and after photo-cross-linking, time-dependent absorbance of Por while binding to the imprinted film with different bulk concentrations of Por, absorbance of Por at 425 nm as a function of bulk concentration of Por, fitting to Langmuir isotherm, and CV characterization of competitive adsorption of Por and redox label into SMI-LbL device. This material is available free of charge via the Internet at http://pubs.acs.org.

## ■ AUTHOR INFORMATION

### Corresponding Author

*E-mail: shi@mail.buct.edu.cn (F.S.); an@cugb.edu.cn (Q.A.).

### Notes

The authors declare no competing financial interest.

## ■ ACKNOWLEDGMENTS

This work was supported by NSFC (21074008), the Program of the Co-Construction with Beijing Municipal Commission of Education of China, Program for New Century Excellent Talents in University (NCET-10-0211), the Fok Ying Tung Education Foundation (131013), the Fundamental Research Funds for the Central Universities (ZZ1104, 2652013115), and Open Project of State Key Laboratory of Supramolecular Structure and Materials (SKLSSM201313).

## ■ REFERENCES

(1) Vlatalkis, G.; Andersson, L. I.; Müller, R.; Mosbach, K. *Nature* **1993**, *361*, 645−647.
(2) Lahav, M.; Katz, E.; Dron, A.; Patolsky, F.; Wilner, I. *J. Am. Chem. Soc.* **1999**, *121*, 862−863.
(3) Riskin, M.; Tel-vered, R.; Bourenko, T.; Granot, E.; Willner, I. *J. Am. Chem. Soc.* **2008**, *130*, 9726−9733.
(4) Frasconi, M.; Tel-vered, R.; Riskin, M.; Willner, I. *J. Am. Chem. Soc.* **2010**, *132*, 9373−9382.
(5) Lee, S.-W.; Ichinose, I.; Kunitake, T. *Langmuir* **1998**, *14*, 2857−2863.
(6) Hu, X.; An, Q.; Li, G.; Tao, S.; Liu, J. *Angew. Chem., Int. Ed.* **2006**, *45*, 8145−8148.
(7) Hu, X.; Huang, J.; Zhang, W.; Li, M.; Tao, C.; Li, G. *Adv. Mater.* **2008**, *20*, 4074−4078.
(8) Wu, Z.; Hu, X.; Tao, C.; Li, Y.; Liu, J.; Yang, C.; Li, G. *J. Mater. Chem.* **2008**, *18*, 5452−5458.
(9) Zhu, W.; Tao, S.; Tao, C.; Li, W.; Lin, C.; Li, M.; Wen, Y.; Li, G. *Langmuir* **2011**, *27*, 8451−8457.
(10) Shi, F.; Liu, Z.; Wu, G.; Zhang, M.; Chen, H.; Wang, Z.; Zhang, X.; Willner, I. *Adv. Funct. Mater.* **2007**, *17*, 1821−1827.
(11) Gauczinski, J.; Liu, Z.; Zhang, X.; Schoenhoff, M. *Langmuir* **2010**, *26*, 10122−10128.
(12) Niu, J.; Liu, Z.; Fu, L.; Shi, F.; Ma, H.; Ozaki, Y.; Zhang, X. *Langmuir* **2008**, *24*, 11988−11994.
(13) Zhang, J.; Liu, Y.; Wu, G.; Schoenhoff, M.; Zhang, X. *Langmuir* **2011**, *27*, 10370−10375.
(14) Liu, Z.; Yi, Y.; Xu, H.; Zhang, X.; Ngo, T. H.; Smet, M. *Adv. Mater.* **2010**, *22*, 2689−2693.
(15) Liu, Z.; Yi, Y.; Gauczinski, J.; Xu, H.; Schoenhoff, M.; Zhang, X. *Langmuir* **2011**, *27*, 11806−11812.
(16) Gauczinski, J.; Liu, Z.; Zhang, X.; Schoenhoff, M. *Langmuir* **2012**, *28*, 4267−4273.
(17) Zhang, X.; Jiang, C.; Cheng, M.; Zhou, Y.; Zhu, X.; Nie, J.; Zhang, Y.; An, Q.; Shi, F. *Langmuir* **2012**, *28*, 7096−7100.
(18) Chen, Y.-W.; Rick, J.; Chou, T. C. *Org. Biomol. Chem.* **2009**, *7*, 488−494.